Search for a new spin-0 scalar and a spin-1 boson using Run2 ATLAS detector data

Xola Mapekula[1], **Simon Connell**[1], **Loan Truong**[1], **Carlos Solans Sanchez**[2]

[1]Department of Mechanical Engineering Science, University of Johannesburg, Johannesburg, South Africa
[2]CERN, Geneva, Switzerland

E-mail: `xola.mapekula@cern.ch`

Abstract. We present a search for a spin-1 boson together with a spin-0 scalar where the additional scalar decays into a four-lepton final state ($\ell = \mu$ or e) via two intermediate dark vector bosons in the following decay channel $S \rightarrow Z_d Z_d \rightarrow 4\ell$. In this scenario, the targeted additional scalar (S) is between 20 GeV and 1 TeV, where we exclude the Higgs boson mass window of 115 GeV $< m_S <$ 130 GeV, while the dark vector boson (Z_d) has a mass between 15 and 300 GeV. The Z_d is assumed to be on-shell, giving rise to the condition $m_{Z_d} < \frac{1}{2} m_S$. The search is conducted using $p-p$ collision data collected using the ATLAS detector at the LHC corresponding to a center of mass energy of $\sqrt{s} = 13$ TeV and an integrated luminosity of 139 fb^{-1}. No significant excesses observed. Therefore, a 95% upper limit was set on the cross-section times branching ratio as a function of the mass of both particles m_S and m_{Z_d}.

1 Introduction

Dark Matter candidates are provided in a group of models that extend the Standard Model (SM) by introducing a $U(1)_d$ symmetry leading to a dark sector as in the Hidden Abelian Higgs Model (HAHM). The dark sector gauge field, postulated in HAHM, contains a $U(1)_d$ gauge symmetry that mixes kinetically with the SM $U(1)_Y$ with a coupling strength of ϵ [1, 2, 3]. This also gives rise to the formation of an additional scalar S, which is a lighter or heavier partner of the SM Higgs boson. The additional scalar and the SM Higgs boson could mix via the Higgs coupling parameter κ. Any production mode of the SM Higgs would also be a production mode of the new scaler. The dominant production mode in (pp) collisions would therefore be via gluon-gluon fusion. Gauge couplings determine the decay of the Z_d. These decays are independent of the values of ϵ, $\kappa \gg 1$. The branching ratio of the dark vector boson would vary between 10% and 15% over the dark vector boson mass range of 1 GeV $< m_{Z_d} <$ 300 GeV. However, the branching ratio falls to 4% in the mass range 60 GeV $< m_{Z_d} <$135 GeV. Figure 1 shows the Feynman diagram of this process.

This study is an extension of previous work where a search for a resonance produced SM Higgs exotically decaying to $Z_d Z_d$ or $Z_d Z$ pairs [4, 5, 6] was performed, where each Z_d decays into either an electron or muon pair with opposite electric charge. These searches used data from the Large Hadron Collider and the ATLAS detector. The beam energies correspondied to$\sqrt{s}$ = 8 TeV and$\sqrt{s}$ = 13 TeV. This work extends the $H \rightarrow Z_d Z_d \rightarrow 4\ell$ search to the case where there is now also a new scalar S and its mass is distinct from the SM Higgs Boson. The search presented in this paper is restricted to the mass region $m_S <$800 GeV and $m_{Z_d} <$300 GeV.

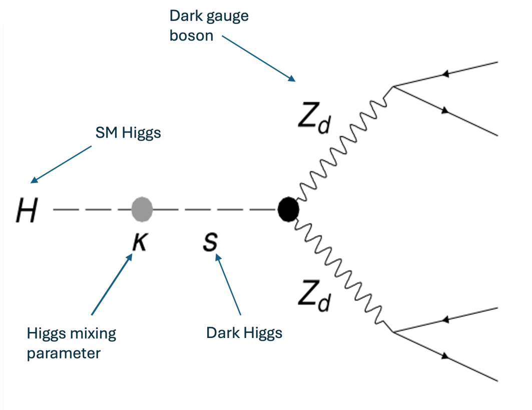

Figure 1: Feymann diagram of an SM Higgs decaying into a pair of dark gauge bosons, via the mixing parameter (κ)

2 ATLAS detector

The ATLAS detector is one of the general-purpose detectors that was designed and built to find the Higgs boson and other physics that lie beyond the SM. The detector captures snapshots of proton-proton (pp) collisions occurring at one of the interaction points located along the LHC's circular path, around which the detector is positioned. The ATLAS detector consists of an Inner Detector, an Electro-magnetic Calorimeter, a Hadronic Calorimeter and a Muon Spectrometer.

The Inner Detector covers the pseudo-rapidity range of $|\eta| < 2.5$. It consists of a silicon microstrip, a silicon pixel and a transition radiation tracker. It measures the trajectory, momentum, and charge of electrically charged particles produced by the collisions. The Electromagnetic and Hadronic Calorimeter are used to measure the energy deposit of particles with high granularity. The Electromagnetic calorimeter takes measurements within the region $|\eta| < 3.2$, while the Hadronic Calorimeters take measurements within the region $|\eta| < 1.7$. The Muon Spectrometer is used to measure the momentum of muons and covers the region $|\eta| < 2.7$.

3 Main Backgrounds

Monte Carlo is used to determine the expected shapes and yields for both signal and background events. Simulations include detector and pileup effects. To account for small differences in isolation and reconstruction impact parameter efficiency, weights are applied to simulated events. Backgrounds comprising systems with four lepton final states are estimated from simulated data 90-95 % of total comes from the dominant $ZZ^\star \to 4\ell$ data. Backgrounds related to SM Higgs production are removed by applying the requirement $m_{4\ell}$ < 115 GeV and $m_{4\ell} >$ 130 GeV. Table 1 shows the list of backgrounds.

Process	ME generator	ME PDF	PS/UE/HF model	UE tune
$H \to Z_d Z_d$	MADGRAPH5 aMC@NLO	NNPDF2.3lo	PYTHIA/EVTGEN	A14
ggF	POWHEG BOX	PDF4LHC15 NNLO	PYTHIA/EVTGEN	AZZNLO
VBF	POWHEG BOX	CT10 NLO	PYTHIA/EVTGEN	AZZNLO
VH	Pythia	NNPDF2.3lo	PYTHIA/EVTGEN	A14
$ggZH$	POWHEG BoX	NNPDF3.0nlo	PYTHIA/EVTGEN	AZZNLO
$b\bar{b}H$	MADGRAPH5 aMC@NLO	NNPDF2.3lo	PYTHIA/EVTGEN	A14
$t\bar{t}H$	POWHEG BOX	NNPDF2.3lo	PYTHIA/EVTGEN	A14
ZZ	SHERPA	NNPDF3.0nnlo	SHERPA	SHERPA default
VVV	SHERPA	NNPDF3.0nnlo	SHERPA	SHERPA default
$t\bar{t}Z$	SHERPA	NNPDF3.0nnlo	SHERPA	SHERPA default
$Z + jets$	SHERPA	NNPDF3.0nnlo	SHERPA	SHERPA default
$t\bar{t}$	POWHEG BOX	NNPDF3.0nlo	PYTHIA/EVTGEN	A14
WZ	POWHEG BOX	CT10 NLO	PYTHIA/EVTGEN	A14

Table 1: Backgrounds

3.1 Signal Simulation

Signal samples with different mass values for S and Z_d were produced in ggH production mode using MadGraph5_aM@NLO v2.2.3. ϵ and κ were adjusted to allow $S \to Z_d Z_d \to 4\ell$ decays were observed. The mass of the dark Higgs was set to be at least twice that of the dark gauge boson. Mass of Dark Higgs varied from below the SM Higgs mass to above the SM Higgs mass. Expected signal distribution shown for SR1 (30 GeV $< m_{4\ell} <$ 115 GeV) and SR2 (130 GeV $< m_{4\ell} <$ 800 GeV) are shown in figure 2.

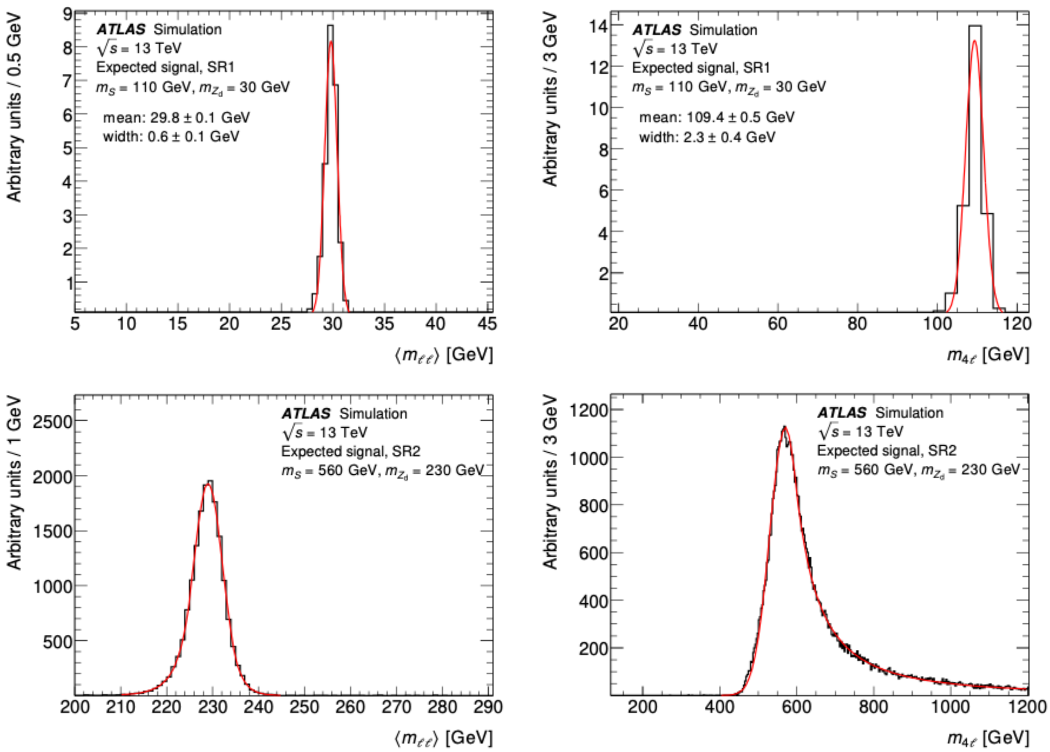

Figure 2: Expected signal distributions for $m_{4\ell}$ and $m_{\ell\ell}$ in the two signal regions SR1 and SR2.

3.2 Event Selection

The electrons and muons are the final-state objects considered in this analysis. The charged particle tracks in the Inner Detector that match energy deposits in the Electromagnetic Calorimeter are used to identify electrons. No more than one Calorimeter Tagged or Standalone muons are allowed to be in an event while the rest must be combined muons. The selection looks for a quadruplet containing two Same Flavour Opposite Sign (SFOS) lepton pairs. The quadruplet with the smallest lepton pair mass difference is chosen. Leptons in a quadruplet must be isolated from other tracks in the ID and energy deposits in the electromagnetic calorimeter. Dilepton pairs formed with either electron or muon pairs are inconsistent with the SM Z-boson mass. Event selection is listed in table 2.

3.3 Results

To obtain the shape of the $m_{\ell\ell}$ distribution in the m_S-$m_{\ell\ell}$ plane, 2D interpolation was used. The number of observed event data are statistically compatible with expected SM background, as listed in table 3. Figure 3 shows the observed data in SR1 and SR2. The horizontal band in SR2 indicates the region excluded by the Z-Veto cut listed in 3.

Group	Cut	Criteria
Electrons	η	|η| < 2.47
	ID	LooseLH working point requirements on silicon and pixel hits
	OQ	Not from a bad cluster
	$z_0 sin\theta$	< 0,5 mm
Muons	p_T	$>$ 6 GeV (15 GeV if calo-tagged)
	η	|η| < 2.47
	ID	Loose
	$z_0 sin\theta$	< 0,5 mm
	$\|d_0\|$	< 1 mm if muon is not stand-alone
Quadruplets	Quadruplet	At least one quadruplet formed from two SFOS dilepton pairs
	Overlap removal	No overlap removed e or μ
	p_T	p_T^1 > 20 GeV, p_T^2 > 15 GeV, p_T^3 > 10 GeV
	Trigger Matched	Leptons in quadruplet responsible for firing at least one trigger
	ΔR	> 0.1 between same-flavor leptons, > 0.2 between different flavor
	Muon Quality	Number of stand-alone or calo-tagged μ < 2
Ranking	Minimal Δm	Select quadruplet pass LooseLH working point
Event selection	Isolation	All leptons in quadruplet pass Fixed-CutLoose working point
	Impact Parameter	$\|d_0^{BL}\|$ < 5(3) for $e(\mu)$ in quadruplet
	Quarkonia Veto	($m_{J/\psi}$ - 0.25 GeV) < $m_{ab}, m_{cd}, m_{ad}, m_{cb}$ < ($m_{\psi(2S)}$ + 0.3 GeV)
		or ($m_{\Upsilon/(1S)}$ - 0.7 GeV) < $m_{ab}, m_{cd}, m_{ad}, m_{cb}$ < ($m_{\Upsilon/(3S)}$ + 0.75 GeV)
	Low mass veto	(m_{ab},m_{cd},m_{ad},m_{cb}) $>$ 5 GeV
	Z veto	$m_{ab} \notin [50, 106]$ GeV for SR1
		m_{ab} and $m_{cd} \notin [83.2, 99.2]$ GeV,
		m_{ab} and $m_{cd} \notin [83.2, 99.2]$ GeV for SR2
	Lose SR	(m_{ab},m_{cd},m_{ad},m_{cb}) $>$ 10 GeV
	H veto	$m_{4\ell} <$ 115 GeV for SR1
		$m_{4\ell} >$ 130 GeV for SR2
	Medium SR	new SR
	Tight SR	$\|E'_{ab}/m_{4\ell} - 0.5\| < 0.008$

Table 2: A list of the event selection cuts used in the analysis

Region	Mass range	Expected yield	Background yield
SR1	($m_{4\ell} <$ 115 GeV)	36	32 $\pm$ 33
SR2	($m_{4\ell} >$ 130 GeV)	55	68 $\pm$ 8

Table 3: Expected and background yields

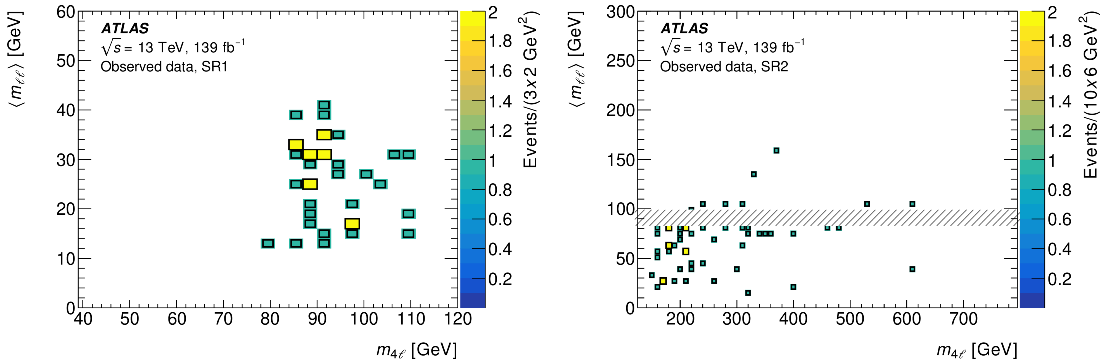

Figure 3: Histogram showing the observed data in both SR1 and SR2 signal regions. The Z Veto exclusion requirement is shown by the horizontal band.

3.4 Limit Setting

The Frequentist approach, CLs, is used to set 95% upper limit on the $\sigma(gg \to S) \times BR(S \to Z_d Z_d \to 4\ell)$ as a function of $m_\ell \ell$ and $m_4 \ell$, as shown in figure 4. In addition, the significance reported as the smallest p-value in SR1 is 2.7σ local, 0.5σ global, at m_S = 110 GeV and m_{Zd} = 30 GeV. The smallest p-value in SR2 is 2.8σ local, 1.6σ global, at m_S = 350 GeV and m_{Zd} = 75 GeV.

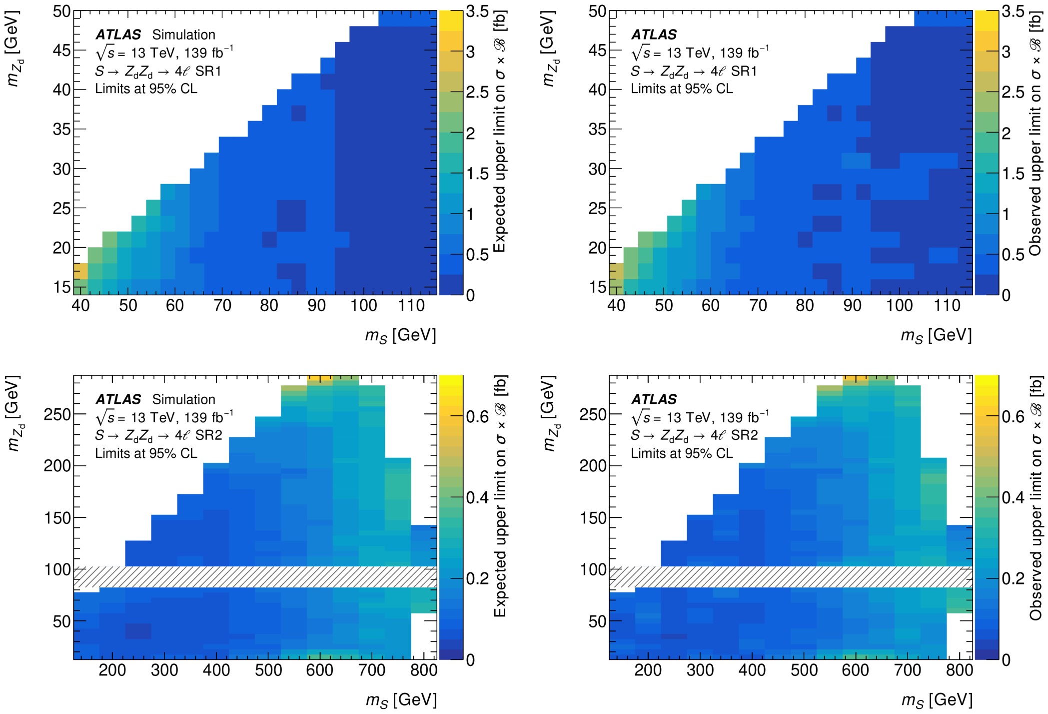

Figure 4: Upper limits on $\sigma(gg \to S) \times BR(S \to Z_d Z_d \to 4\ell)$ for $m_{4\ell}$ and $m_{\ell\ell}$ in the two signal regions SR1 and SR2.

3.5 Conclusions

The analysis investigates the decay of a new spin-0 scalar particle, S, decaying into a four-lepton final state via two promptly decaying spin-1 bosons $S \to Z_d Z_d$, with each Z_d boson decaying promptly into a pair of electrons or muons. The study examines two distinct signal regions: one with 30 GeV $< m_{4\ell} <$ 115 GeV and another with

130 GeV $< m_{4\ell} <$ 800 GeV. The results show that the data are consistent with the Standard Model background expectations, and 95% confidence level (CL) upper limits are placed on the total cross section times branching ratio. $\sigma(gg \to S) \times BR(S \to Z_d Z_d \to 4\ell)$ as a function of $m_{\ell\ell}$ and $m_{4\ell}$. These limits constrain the dark sector predicted by the Hidden Abelian Higgs Model.

References

[1] H. Davoudiasl, H.-S. Lee, I. Lewis, and W. J. Marciano, "Higgs decays as a window into the dark sector," *Physical Review D*, vol. 88, no. 1, p. 015022, 2013.

[2] D. Curtin, R. Essig, and Y.-M. Zhong, "Uncovering light scalars with exotic higgs decays to $b\bar{b}\mu^+\mu^-$," *Journal of High Energy Physics*, vol. 2015, no. 6, p. 25, 2015.

[3] H. Davoudiasl, H.-S. Lee, and W. J. Marciano, ""dark" z implications for parity violation, rare meson decays, and higgs physics," *Physical Review D*, vol. 85, no. 11, p. 115019, 2012.

[4] ATLAS Collaboration, "Search for Higgs bosons decaying into new spin-0 or spin-1 particles in four-lepton final states with the ATLAS detector with $139\,\text{fb}^{-1}$ of pp collision data at $\sqrt{s} = 13\,\text{TeV}$," *JHEP*, vol. 03, p. 041, 2022.

[5] ATLAS collaboration, "Search for Higgs boson decays to beyond the Standard Model light bosons in four-lepton events with the ATLAS detector at $\sqrt{s} = 13\,\text{TeV}$," *JHEP*, vol. 06, p. 166, 2018.

[6] ATLAS Collaboration, "Search for new light gauge bosons in Higgs boson decays to four-lepton final states in pp collisions at $\sqrt{s} = 8\,\text{TeV}$ with the ATLAS detector at the LHC," *Phys. Rev. D*, vol. 92, p. 092001, 2015.